- Supramolecular Interactions of High Molecular Weight Poly(2,7-carbazole)s with Single-Walled Carbon Nanotubes
  Rice, N. A.; Adronov, A.. *Macromolecules* **2013**, *46*, 3850-3860.
  Abstract:

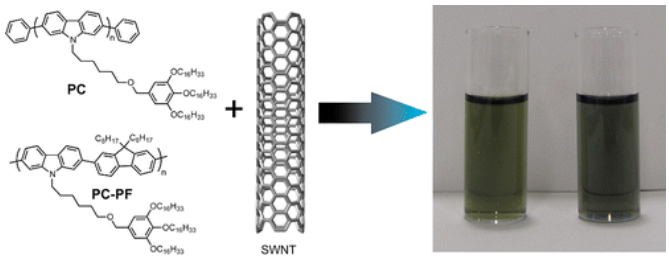

A novel 2,7-carbazole monomer unit was synthesized and used to prepare two poly(2,7-carbazole)s, both of which were obtained in relatively high molecular weight and display excellent solubility in common organic solvents. The polymers were able to effectively disperse carbon nanotube bundles in both THF and toluene using a relatively simple procedure to yield concentrated polymer-carbon nanotube samples that were stable for months. The polymer-coated carbon nanotube samples were characterized by thermogravimetric analysis, atomic force microscopy, absorption spectroscopy, photoluminescence mapping, and Raman spectroscopy. It was found that the polymers used in this study preferentially interact with carbon nanotubes having diameters of 1.15 nm or less. Additionally, it was observed that the carbon nanotubes remained effectively debundled by the polymers after removal of solvent, as was demonstrated by Raman and photoluminescence mapping of solid films of the polymer-carbon nanotube composites.

- Ring-Opening Metathesis Polymerization by a Ru Phosphine Derivative of Cyclodextrin in Water
  Takashima, Y.; Uramatsu, K.; Jomori, D.; Harima, A.; Otsubo, M.; Yamaguchi, H.; Harada, A. *ACS Macro Lett*. **2013**, *2*, 384-387.
  Abstract:

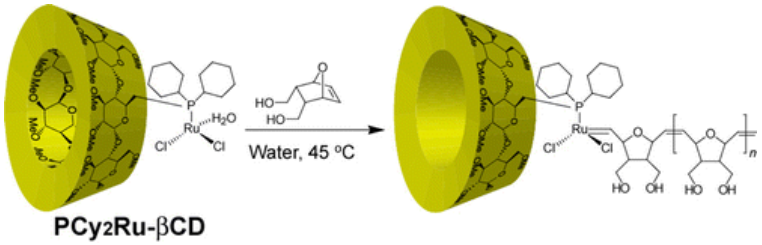

Trimethylated cyclodextrins with a phosphine ligand and ruthenium (PCy_2Ru-CDs) realize supramolecular polymerization catalysts for ring-opening metathesis polymerization (ROMP). Although PCy_2Ru-βCD shows a low polymerization activity for 7-oxanorbornene dimethanol (7-$ONorOH_2$) in organic solvents, it exhibits a high ROMP activity for 7-$ONorOH_2$ in aqueous solutions. The ROMP activity of PCy_2Ru-βCD is higher than that of PCy_2Ru-αCD. The addition of competitive guest molecules decreases the polymer yield, indicating that complexation between PCy_2Ru-CD and 7-$ONorOH_2$ in water plays an important role in the increased polymer yield.

- Thermoresponsive self-assembled polymer colloids in water
  Hocine, S.; Li, M.-H. *Soft Matter* **2013,** *9*, 5839-5861.
  Abstract:

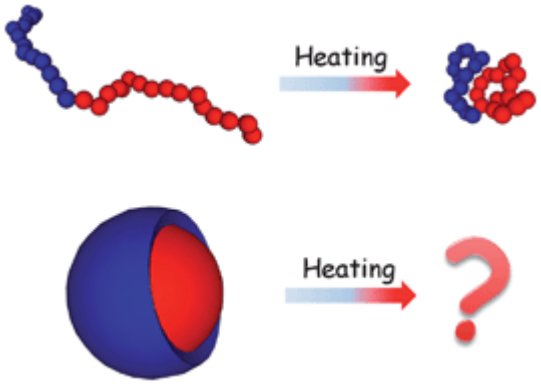

Thermoresponsive polymer colloids made of amphiphilic block copolymers are reviewed in this paper. The main families of thermoresponsive polymers, including hydrophilic polymers with LCST (PEG, PNIPAM, poly(oxazoline)s and elastin-like polypeptides, *etc.*) and hydrophobic polymers with thermotropic phase transitions (liquid crystalline and crystalline polymers), are first described with the details of the underlying physical chemical principles. Polymer colloids with thermoresponsive polymers as the hydrophobic core, hydrophilic corona or both of them depending on temperature (*schizophrenic systems*) are discussed and their potential bio-related applications highlighted. We also take notice of the particular thermoresponsive properties of PEG in the polymer colloids. Hydrophilic PEG has its water solubility and degree of hydration decreased with increasing temperature in the range far below its LCST (~100 °C). These properties can result in significant or even drastic morphological changes in colloids, which should be taken into account when designing thermoresponsive polymer colloids using the PEG corona.

- Responsive organogels formed by supramolecular self assembly of PEG-block-allyl-functionalized racemic polypeptides into [small beta]-sheet-driven polymeric ribbons
  Zou, J.; Zhang, F.; Chen, Y.; Raymond, J. E.; Zhang, S.; Fan, J.; Zhu, J.; Li, A.; Seetho, K.; He, X.; Pochan, D. J.; Wooley, K. L. *Soft Matter* **2013,** *9*, 5951-5958.
  Abstract:

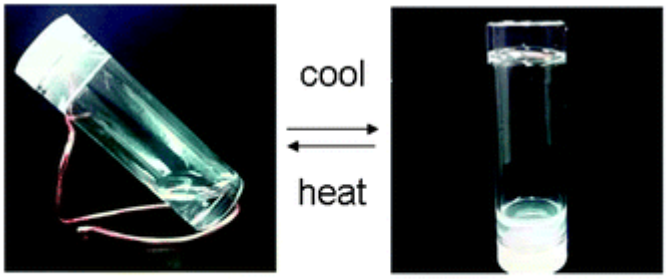

$mPEG_{112}$-*b*-Poly(DL-allylglycine)$_{12}$
Concentration = 1 mg/mL (0.1 wt %)

A chemically reactive hybrid diblock polypeptide gelator poly(ethylene glycol)-*block*-poly(DL-allylglycine) (PEG-*b*-PDLAG) is an exceptional material, due to the characteristics of thermo-reversible organogel formation driven by the combination of a hydrophilic polymer chain linked to a racemic oligomeric homopeptide segment in a range of organic solvents. One-dimensional stacking of the block copolymers is demonstrated by ATR-FTIR spectroscopy, wide-angle X-ray scattering to be driven by the supramolecular assembly of β-sheets in peptide blocks to afford well-defined fiber-like structures, resulting in gelation. These supramolecular interactions are sufficiently strong to achieve ultra low critical gelation concentrations (*ca.* 0.1 wt%) in *N*,*N*-dimethylformamide (DMF), dimethyl

sulfoxide (DMSO) and methanol. The critical gel transition temperature was directly proportional to the polymer concentration, so that at low concentrations, thermoreversibility of gelation was observed. Dynamic mechanical analysis studies were employed to determine the organogel mechanical properties, having storage moduli of *ca.* 15.1 kPa at room temperature.

- A Bioinspired Approach for Shaping Au Nanostructures: The Role of Biomolecule Structures in Shape Evolution
  Sahu, S. C.; Samantara, A. K.; Ghosh, A.; Jena, B. K. *Chem. Eur. J.* **2013**, *25*, 8220-8226.
  Abstract:

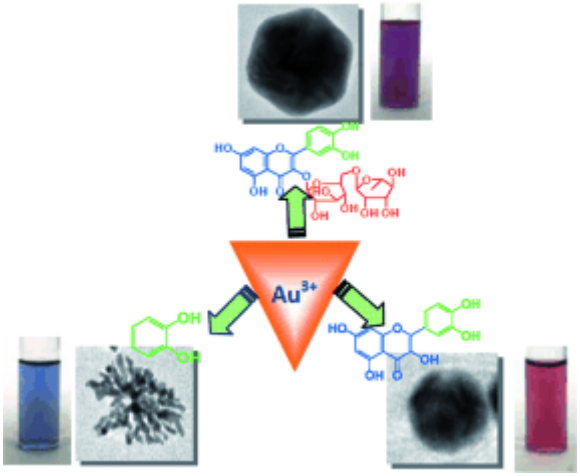

A new approach for shaping Au nanostructures by tuning the molecular structure of biomolecules has been explored. Different molecules, such as catechol, rutin, and quercetin, which have structural similarity to the catechol ring, were used to induce Au nanostructures under similar conditions. The as-synthesized nanostructures are characterized by using TEM, XPS, XRD, and UV/Vis spectral measurements. The growth mechanism for the formation of these noble metal shapes and the role of the molecular structure of the stabilizing/reducing agent were investigated by using TEM and UV/Vis spectral measurements. The structure and functional groups of the reducing/stabilizing agent play a vital role in the shape evolution of nanostructures. The electrocatalytic activity of different nanostructures in the reduction of oxygen was investigated and was found to be shape-dependent.

- Columnar Self-Assembly in Electron-Deficient Heterotriangulenes
  Kivala, M.; Pisula, W.; Wang, S.; Mavrinskiy, A.; Gisselbrecht, J.-P.; Feng, X.; Müllen, K. *Chem. Eur. J.* **2013**, *25*, 8117-8128.
  Abstract:

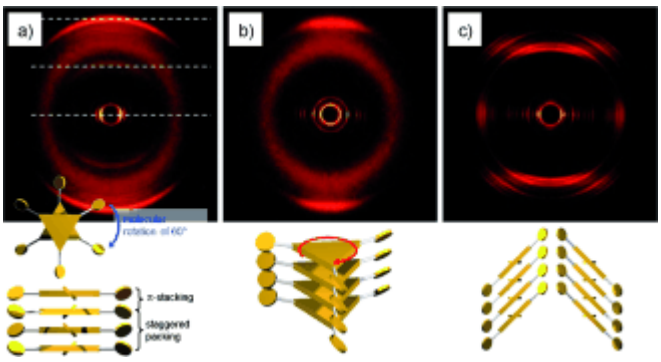

A series of soluble carbonyl-bridged heterotriangulenes, in which flexible *n*-dodecyl chains are attached through different spacers to the planar nitrogen-centered polycyclic core, have been

synthesized. The introduction of triisopropylsilylethynyl moieties enabled, for the first time, the characterization of single-crystal columnar packing of a substituted heterotriangulene by X-ray crystallography. Electrochemical studies disclosed the carbonyl-bridged heterotriangulene core as a reasonably strong acceptor for a reversible two-electron transfer. The tendency of substituted heterotriangulenes to self-assemble in solution, on surfaces, and in the bulk appeared to sensitively depend on the nature of the lateral substituents, their steric demand, and the applied solution processing conditions. It can be concluded that 1) additional phenylene moieties between the heterotriangulene core and the *n*-dodecyl chains facilitate self-assembly by extending the π-conjugated polycyclic disc, 2) the rod-like ethynylene spacers introduce some additional flexibility and hence lower the overall aggregation tendency, and 3) the combination of both features in the phenylene–ethynylene moieties induces thermotropic liquid crystallinity.

- Multifunctional Semiconductor Nanoheterostructures via Site-Selective Silica Encapsulation
  Xu, Y. ; Lian, J.; Mishra, N.; Chan, Y. *Small* **2013**, *9*, 1908–1915.
  Abstract:

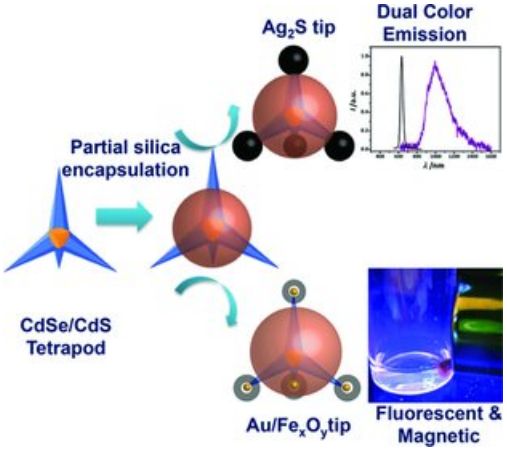

Site-specific silica encapsulation of the CdSe core region of CdSe/CdS tetrapods is employed to allow for the fluorescence from the CdSe core to be preserved during the growth of secondary functional materials, which is exploited to achieve Ag_2S-tipped SiO_2-CdSe/CdS tetrapods with dual emission at visible and IR wavelengths and Au/Fe_xO_y-tipped SiO_2-CdSe/CdS tetrapods which exhibits both fluorescence and a strong magnetic response.

- Charge Transfer at Junctions of a Single Layer of Graphene and a Metallic Single Walled Carbon Nanotube
  Paulus, G. L. C.; Wang, Q. H.; Ulissi, Z. W.; McNicholas, T. P.; Vijayaraghavan, A.; Shih, C-J.; Jin, Z.; Strano, M. S. *Small* **2013**, *9*, 1954–1963.
  Abstract:

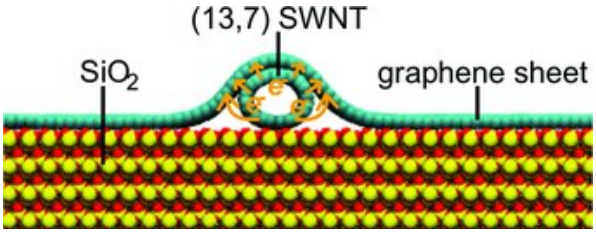

Junctions between a single walled carbon nanotube (SWNT) and a monolayer of graphene are fabricated and studied for the first time. A single layer graphene (SLG) sheet grown by chemical vapor deposition (CVD) is transferred onto a SiO_2/Si wafer with aligned CVD-grown SWNTs. Raman

spectroscopy is used to identify metallic-SWNT/SLG junctions, and a method for spectroscopic deconvolution of the overlapping G peaks of the SWNT and the SLG is reported, making use of the polarization dependence of the SWNT. A comparison of the Raman peak positions and intensities of the individual SWNT and graphene to those of the SWNT-graphene junction indicates an electron transfer of 1.12×10^{13} cm^{-2} from the SWNT to the graphene. This direction of charge transfer is in agreement with the work functions of the SWNT and graphene. The compression of the SWNT by the graphene increases the broadening of the radial breathing mode (RBM) peak from 3.6 ± 0.3 to 4.6 ± 0.5 cm^{-1} and of the G peak from 13 ± 1 to 18 ± 1 cm^{-1}, in reasonable agreement with molecular dynamics simulations. However, the RBM and G peak position shifts are primarily due to charge transfer with minimal contributions from strain. With this method, the ability to dope graphene with nanometer resolution is demonstrated.

- A Smart DNA Tetrahedron That Isothermally Assembles or Dissociates in Response to the Solution pH Value Changes
  Liu, Z.; Li, Y.; Tian, C.; Mao, C. *Biomacromolecules* **2013**, *14*, 1711-1714.
  Abstract:

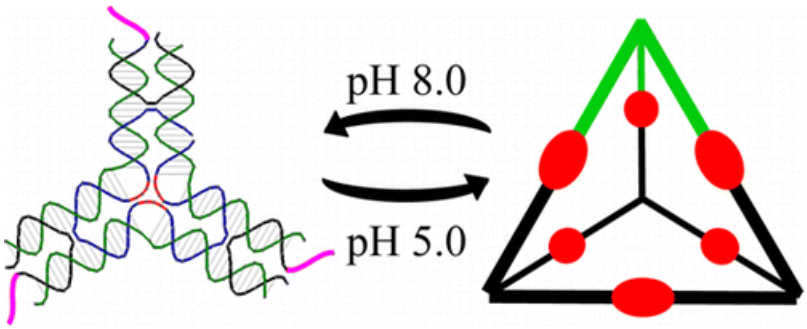

This communication reports a DNA tetrahedron whose self-assembly is triggered by an acidic environment. The key element is the formation/dissociation of a short, cytosine (C)-containing, DNA triplex. As the solution pH value oscillates between 5.0 and 8.0, the DNA triplex will form and dissociate that, in turn, leads to assembly or disassembly of the DNA tetrahedron, which has been demonstrated by native polyacrylamide gel electrophoresis (PAGE). We believe that such environment-responsive behavior will be important for potential applications of DNA nanocages such as on-demand drug release.

- Magnetic Porous Sugar-Functionalized PEG Microgels for Efficient Isolation and Removal of Bacteria from Solution
  Behra, M.; Azzouz, N.; Schmidt, S.; Volodkin, D. V.; Mosca, S.; Chanana, M.; Seeberger, P. H.; Hartmann, L. *Biomacromolecules* **2013**, *14*, 1927-1935.
  Abstract:

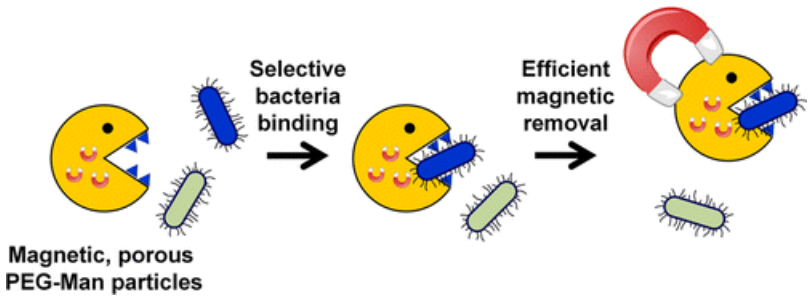

Here, we present a new microparticle system for the selective detection and magnetic removal of

bacteria from contaminated solutions. The novelty of this system lies in the combination of a biocompatible scaffold reducing unspecific interactions with high capacity for bacteria binding. We apply highly porous poly(ethylene glycol) (PEG) microparticles and functionalize them, introducing both sugar ligands for specific bacteria targeting and cationic moieties for electrostatic loading of superparamagnetic iron oxide nanoparticles. The resulting magnetic, porous, sugar-functionalized (MaPoS) PEG microgels are able to selectively bind and discriminate between different strains of bacteria *Escherichia coli*. Furthermore, they allow for a highly efficient removal of bacteria from solution as their increased surface area can bind three times more bacteria than nonporous particles. All in all, MaPoS particles represent a novel generation of magnetic beads introducing for the first time a porous, biocompatible and easy to functionalize scaffold and show great potential for various biotechnological applications.

- Enhanced Photoluminescence of Sulfur-Bridged Organic Chromophores
  Christensen, P. R.; Nagle, J. K.; Bhatti, A.; Wolf, M. O. *J. Am. Chem. Soc.* **2013**, *135*, 8109–8112.
  Abstract:

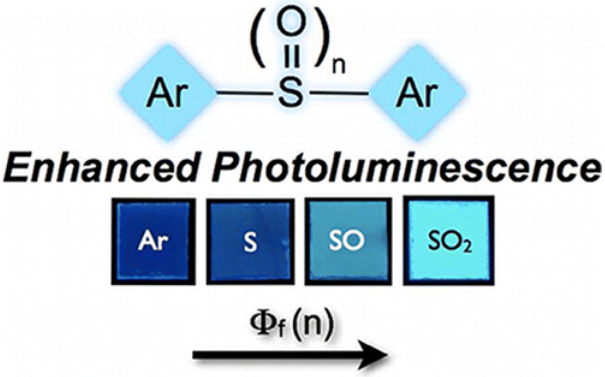

A general approach to enhancing the emission quantum yield of several widely studied organic chromophores is presented. The luminescence properties of a series of symmetrical sulfur-bridged chromophores are reported as a function of the oxidation state of the bridging sulfur atom. The photoluminescence quantum yield is significantly enhanced by successively oxidizing the sulfur bridge from sulfide (S), to sulfoxide (SO), to sulfone (SO_2).

- Dis-assembly of a Benzylic CF_3 Group Mediated by a Niobium(III) Imido Complex
  Gianetti, T. L.; Bergman, R. G.; Arnold, J. *J. Am. Chem. Soc.* **2013,** *135*, 8145–8148.
  Abstract:

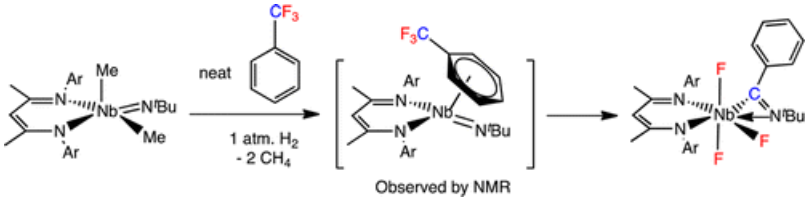

All three C–F bonds in CF_3-substituted arenes are activated by a niobium imido complex, driven by the formation of strong Nb–F bonds. The mechanism of this transformation was studied by NMR spectroscopy, which revealed the involvement of Nb(III). Attempts to extend this chemistry to nonaromatic CF_3 groups led to intramolecular reactivity.

- Cooperative Self-Assembly of Discoid Dimers: Hierarchical Formation of Nanostructures with

a pH Switch

Fenske, M.T.; Meyer-Zaika, W.; Korth, H.-G.; Vieker, H.; Turchanin, A.; Schmuck, C. *J. Am. Chem. Soc.* **2013**, *135,* 8342–8349.

Abstract:

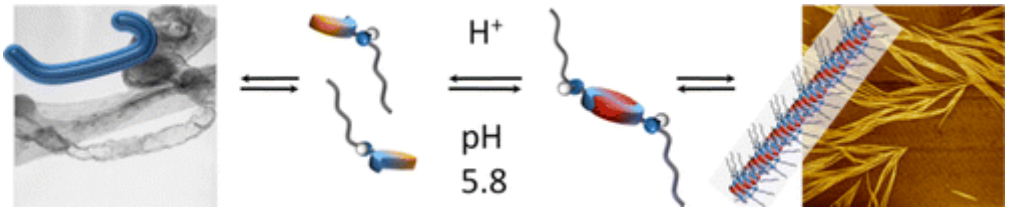

Derivatives of the self-complementary 2-guanidiniocarbonyl pyrrole 5-carboxylate zwitterion (1) (previously reported by us to dimerize to 1•1 with an aggregation constant of ca. >1010 M–l in DMSO) aggregate in a diverse manner depending on, e.g., variation of concentration or its protonation state. The mode of aggregation was analyzed by spectroscopic (NMR, UV) and microscopic (AFM, SEM, HIM, and TEM) methods. Aggregation of dimers of these zwitterions to higher supramolecular structures was achieved by introduction of sec-amide substituents at the 3-position, i.e., at the rearward periphery of the parent binding motif. A butyl amide substituent as in 2b enables the discoid dimers to further aggregate into one-dimensional (rod-like) stacks. Quantitative UV dilution studies showed that this aggregation is strongly cooperative following a nucleation elongation mechanism. The amide hydrogen seems to be essential for this rod-like aggregation, as neither 1 nor a corresponding tert-amide congener 2a form comparable structures. Therefore, a hydrogen bond-assisted π–π-interaction of the dimeric zwitterions is suggested to promote this aggregation mode, which is further affected by the nature of the amide substituent (e.g., steric demand), enabling the formation of bundles of strands or even two-dimensional sheets. By exploiting the zwitterionic nature of the aggregating discoid dimers, a reversible pH switch was realized: dimerization of all compounds is suppressed by protonation of the carboxylate moiety, converting the zwitterions into typical cationic amphiphiles. Accordingly, typical nanostructures like vesicles, tubes, and flat sheets are formed reversibly under acidic conditions, which reassemble into the original rod-like aggregates upon readjustment to neutral pH.

- Photoisomerization Quantum Yield of Azobenzene-Modified DNA Depends on Local Sequence

  Yan, Y.; Wang, X.; Chen, J. I. L.; Ginger, D. S. *J. Am. Chem. Soc.* **2013**, *135,* 8382–8387.

  Abstract:

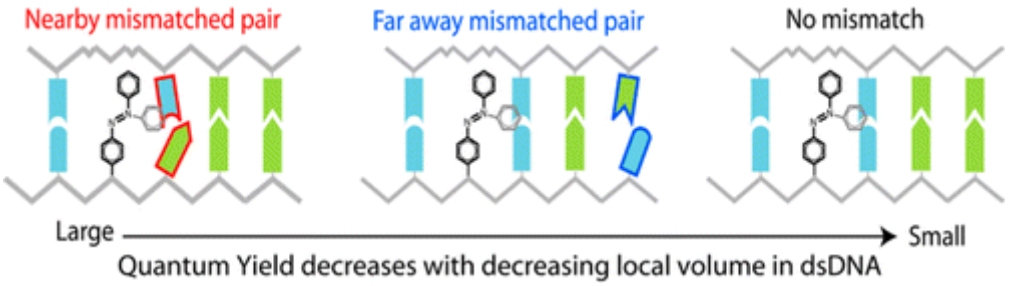

Photoswitch-modified DNA is being studied for applications including light-harvesting molecular motors, photocontrolled drug delivery, gene regulation, and optically mediated assembly of plasmonic metal nanoparticles in DNA-hybridization assays. We study the sequence and hybridization dependence of the photoisomerization quantum yield of azobenzene attached to DNA via the popular d-threoninol linkage. Compared to free azobenzene we find that the quantum yield for

photoisomerization from trans to cis form is decreased 3-fold (from 0.094 ± 0.004 to 0.036 ± 0.002) when the azobenzene is incorporated into ssDNA, and is further reduced 15-fold (to 0.0056 ± 0.0008) for azobenzene incorporated into dsDNA. In addition, we find that the quantum yield is sensitive to the local sequence including both specific mismatches and the overall sequence-dependent melting temperature (Tm). These results serve as design rules for efficient photoswitchable DNA sequences tailored for sensing, drug delivery, and energy-harvesting applications, while also providing a foundation for understanding phenomena such as photonically controlled hybridization stringency.

- Formation of stimuli-responsive supramolecular polymeric assemblies via orthogonal metal–ligand and host–guest interactions
  Ding, Y.; Wang, P.; Tian, Y.; Tian, Y.; Wang, F. *Chem. Commun*. **2013**, *49*, 5951-5953.
  Abstract:

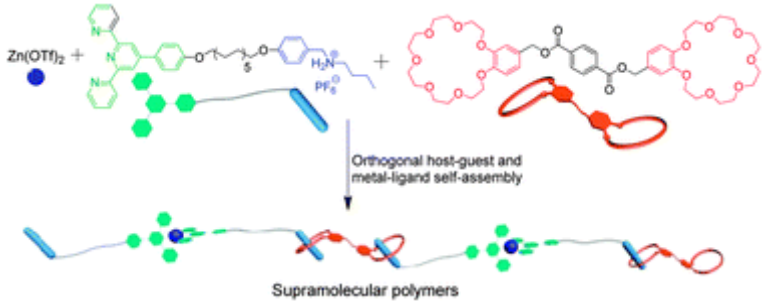

Linear supramolecular polymers, assembled via the combination of orthogonal terpyridine–Zn2+ and benzo-21-crown-7/secondary ammonium salt recognition motifs, exhibit dynamic properties responsive to various external stimuli.

- One-step synthesis of imidazoline-containing macrocycles and their complexation with fullerenes C60 and C7
  Yang, F.; Wang, Z.; Song, F.; Liu, X.; Lan, J.; You, J. *Chem. Commun*. **2013**, *49*, 5975-5977.
  Abstract:

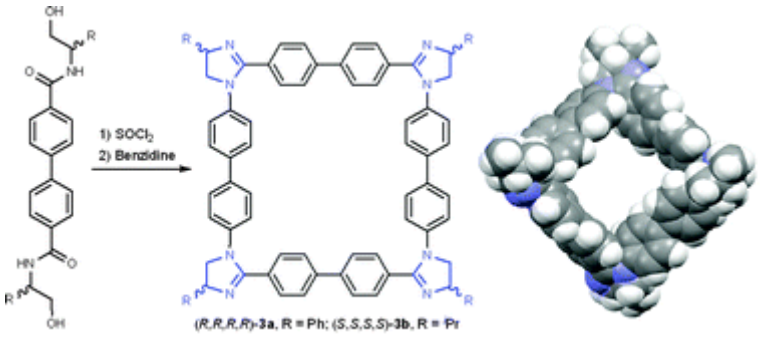

A new family of imidazoline–arylene macrocycles have been constructed through the simultaneous formation of four imidazoline rings in one step. These macrocycles can efficiently complex with fullerenes C_{60} and C_{70} through the formation of ground-state complexes.

- Synthesis of [2]Rotaxanes by the Copper-Mediated Threading Reactions of Aryl Iodides with Alkynes
  Ugajin, K.; Takahashi, E.; Yamasaki, R.; Mutoh, Y.; Kasama, T.; Saito; S. *Org. Lett.* **2013**, *15,* 2684-2687.
  Abstract:

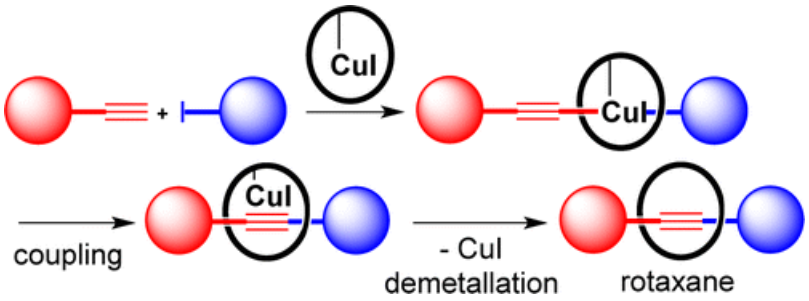

The catalytic activity of the macrocyclic phenanthroline copper(I) complex is utilized for the Sonogashira-type reaction to synthesize [2]rotaxanes. Thus, [2]rotaxanes were prepared by reactions between terminal alkynes and aryl iodides in the presence of the macrocyclic copper complex. Bulky substituents were introduced to the substrates to stabilize the rotaxane. The bond-forming reaction proceeded selectively inside the macrocyclic complex so that the rotaxanes could be synthesized.

- Expansion of Orifices of Open C_{60} Derivatives and Formation of an Open $C_{59}S$ Derivative by Reaction with Sulfur
  Futagoishi, T.; Murata, M.; Wakamiya, A.; Sasamori, T.; Murata, Y. *Org. Lett.* **2013**, *15,* 2750-2753.
  Abstract:

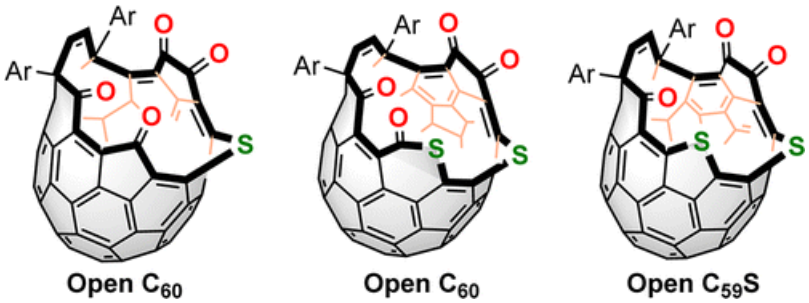

The reaction of a tetraketo-open-cage C_{60} derivative with elemental sulfur in the presence of tetrakis(dimethylamino)ethylene afforded novel open C_{60} derivatives containing sulfur atom(s) in the rim of the orifice and the first example of an open $C_{59}S$ derivative. The single crystal X-ray analyses clearly determined these structures and demonstrated that a water molecule was encapsulated inside the cages. The orifice sizes and electronic properties of these fullerene derivatives were revealed.

- Interplay of physics and evolution in the likely origin of protein biochemical function
  Skolnick, J.; Gao, M. *Proc. Nat. Acad. Sci. USA* **2013**, *110*, 9344-9349.
  Abstract:

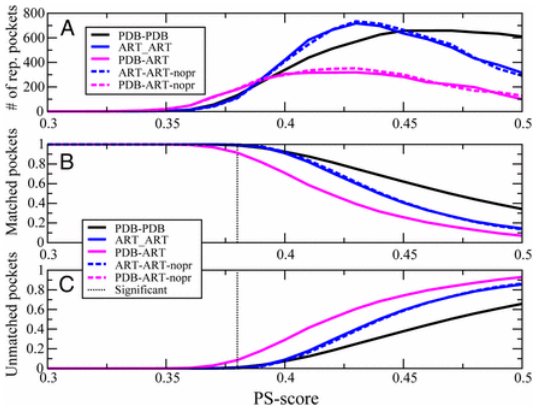

The intrinsic ability of protein structures to exhibit the geometric and sequence properties required for ligand binding without evolutionary selection is shown by the coincidence of the properties of pockets in native, single domain proteins with those in computationally generated, compact homopolypeptide, artificial (ART) structures. The library of native pockets is covered by a remarkably small number of representative pockets (~400), with virtually every native pocket having a statistically significant match in the ART library, suggesting that the library is complete. When sequences are selected for ART structures based on fold stability, pocket sequence conservation is coincident to native. The fact that structurally and sequentially similar pockets occur across fold classes combined with the small number of representative pockets in native proteins implies that promiscuous interactions are inherent to proteins. Based on comparison of PDB (real, single domain protein structures found in the Protein Data Bank) and ART structures and pockets, the widespread assumption that the co-occurrence of global structure, pocket similarity, and amino acid conservation demands an evolutionary relationship between proteins is shown to significantly underestimate the random background probability. Indeed, many features of biochemical function arise from the physical properties of proteins that evolution likely fine-tunes to achieve specificity. Finally, our study suggests that a repertoire of thermodynamically (marginally) stable proteins could engage in many of the biochemical reactions needed for living systems without selection for function, a conclusion with significant implications for the origin of life.

- Coupling a Single Trapped Atom to a Nanoscale Optical Cavity
  Thompson, J. D.; Tiecke, T. G.; de Leon, N. P.; Feist, J.; Akimov, A. V.; Gullans, M.; Zibrov, A. S.; Vuletić, V.; Lukin, M. D. *Science* **2013**, *340*, 1202-1205.
  Abstract:

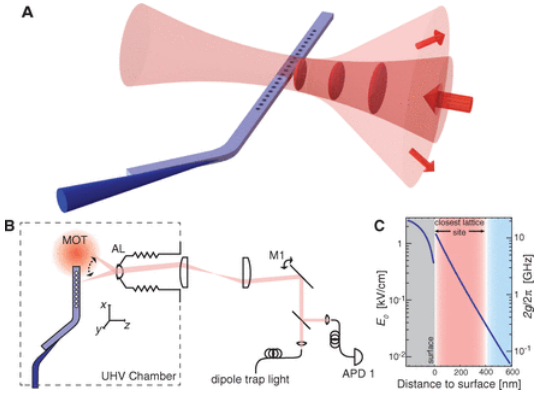

Hybrid quantum devices, in which dissimilar quantum systems are combined in order to attain qualities not available with either system alone, may enable far-reaching control in quantum measurement, sensing, and information processing. A paradigmatic example is trapped ultracold atoms, which offer excellent quantum coherent properties, coupled to nanoscale solid-state systems, which allow for strong interactions. We demonstrate a deterministic interface between a single trapped rubidium atom and a nanoscale photonic crystal cavity. Precise control over the atom's position allows us to probe the cavity near-field with a resolution below the diffraction limit and to observe large atom-photon coupling. This approach may enable the realization of integrated, strongly coupled quantum nano-optical circuits.

- Molecule–electrode interfaces in molecular electronic devices
  Jiaa, C.; Guo, X. *Chem. Soc. Rev.* **2013**, *42*, 5642-5660.

Abstract:

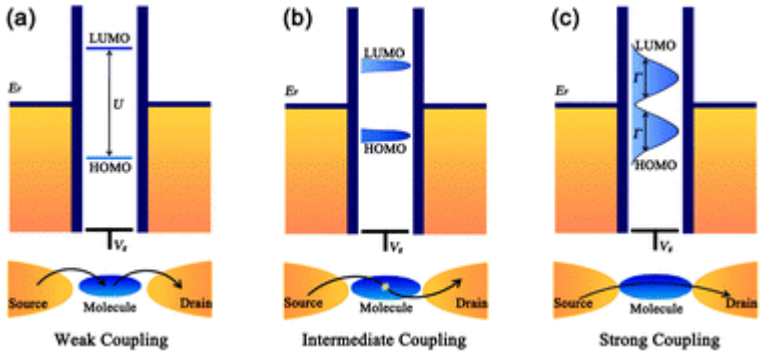

Understanding charge transport of single molecules or a small collection of molecules sandwiched between electrodes is of fundamental importance for molecular electronics. This requires the fabrication of reliable devices, which depend on several factors including the testbed architectures used, the molecule number and defect density being tested, and the nature of the molecule–electrode interface. On the basis of significant progresses achieved in both experiments and theory over the past decade, in this *tutorial review*, we focus on new insights into the influence of the nature of the molecule–electrode interface, the most critical issue hindering the development of reliable devices, on the conducting properties of molecules. We summarize the strategies developed for controlling the interfacial properties and how the coupling strength between the molecules and the electrodes modulates the device properties. These analyses should be valuable for deeply understanding the relationship between the contact interface and the charge transport mechanism, which is of crucial importance for the development of molecular electronics, organic electronics, nanoelectronics, and other interface-related optoelectronic devices.

- Probing excited electronic states and ionisation mechanisms of fullerenes
  Johansson, J. O.; Campbell, E. E. B. *Chem. Soc. Rev.* **2013**, *42*, 5661–5671.
  Abstract:

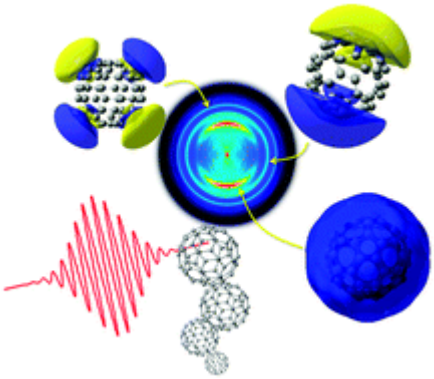

Fullerenes are interesting model systems for probing the complex, fundamental electron dynamics and ionisation mechanisms of large molecules and nanoparticles. In this Tutorial Review we explain how recent experimental and theoretical advances are providing insight into the interesting phenomenon of thermal electron emission from molecular systems and the properties of hydrogenic, diffuse, excited electronic states, known as superatom molecular orbitals, which are responsible for relatively simple, well-resolved structure in fs laser photoelectron spectra of fullerenes. We focus on the application of velocity map imaging combined with fs laser photoionisation to study angular-resolved photoelectron emission.

- A transparent electrode based on a metal nanotrough networks
  Wu, H.; Kong, D.; Ruan, Z.; Hsu, P.-C.; Wang, S.; Yu, Z.; Carney, T. J.; Hu, L.; Fan, S.; Cui, Y. *Nature Nano* **2013**, *8*, 421–425.
  Abstract:

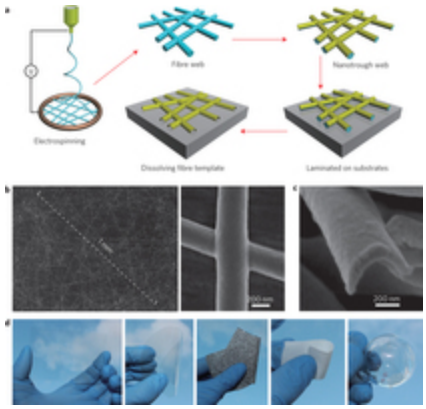

Transparent conducting electrodes are essential components for numerous flexible optoelectronic devices, including touch screens and interactive electronics. Thin films of indium tin oxide—the prototypical transparent electrode material—demonstrate excellent electronic performances, but film brittleness, low infrared transmittance and low abundance limit suitability for certain industrial applications. Alternatives to indium tin oxide have recently been reported and include conducting polymers, carbon nanotubes and graphene. However, although flexibility is greatly improved, the optoelectronic performance of these carbon-based materials is limited by low conductivity. Other examples include metal nanowire-based electrodes, which can achieve sheet resistances of less than $10\Omega\,\square^{-1}$ at 90% transmission because of the high conductivity of the metals. To achieve these performances, however, metal nanowires must be defect-free, have conductivities close to their values in bulk, be as long as possible to minimize the number of wire-to-wire junctions, and exhibit small junction resistance. Here, we present a facile fabrication process that allows us to satisfy all these requirements and fabricate a new kind of transparent conducting electrode that exhibits both superior optoelectronic performances (sheet resistance of $\sim 2\Omega\,\square^{-1}$ at 90% transmission) and remarkable mechanical flexibility under both stretching and bending stresses. The electrode is composed of a free-standing metallic nanotrough network and is produced with a process involving electrospinning and metal deposition. We demonstrate the practical suitability of our transparent conducting electrode by fabricating a flexible touch-screen device and a transparent conducting tape.

- Rubrene-Based Single-Crystal Organic Semiconductors: Synthesis, Electronic Structure, and Charge-Transport Properties
  McGarry, K. A.; Xie, W.; Sutton, C.; Risko, C.; Wu, Y.; Young, Jr., V. G.; Brédas, J.-L.; Frisbie, C. D.; Douglas, C. J. *Chem. Mater.* **2013,** *25*, 2254-2263.
  Abstract:

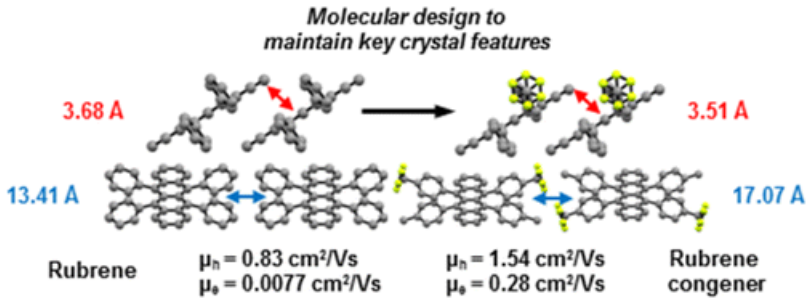

Correlations among the molecular structure, crystal structure, electronic structure, and charge-carrier transport phenomena have been derived from six congeners (**2**–**7**) of rubrene (**1**). The congeners were synthesized via a three-step route from known 6,11-dichloro-5,12-tetracenedione. After crystallization, their packing structures were solved using single-crystal X-ray diffraction. Rubrenes **5**–**7** maintain the orthorhombic features of the parent rubrene (**1**) in their solid-state packing structures. Control of the packing structure in **5**–**7** provided the first series of systematically manipulated rubrenes that preserve the π-stacking motif of **1**. Density functional theory calculations were performed at the B3LYP/6-31G(d,p) level of theory to evaluate the geometric and electronic structure of each derivative and reveal that key properties of rubrene (**1**) have been maintained. Intermolecular electronic couplings (transfer integrals) were calculated for each derivative to determine the propensity for charge-carrier transport. For rubrenes **5**–**7**, evaluations of the transfer integrals and periodic electronic structures suggest these derivatives should exhibit transport characteristics equivalent to, or in some cases improved on, those of the parent rubrene (**1**), as well as the potential for ambipolar behavior. Single-crystal field-effect transistors were fabricated for **5**–**7**, and these derivatives show ambipolar transport as predicted. Although device architecture has yet to be fully optimized, maximum hole (electron) mobilities of 1.54 (0.28) $cm^2\ V^{-1}\ s^{-1}$ were measured for rubrene **5**. This work lays a foundation to improve our understanding of charge-carrier transport phenomena in organic single-crystal semiconductors through the correlation of designed molecular and crystallographic changes to electronic and transport properties.

- Cation, Vacancy, and Spin Ordered 15R-Superstructures in $Sr(Cr_{1-x}Fe_x)O_{3-y}$ ($0.4 \le x \le 0.6$) Perovskites
  Arévalo-López, A. M.; Sher, F.; Farnham, J.; Watson, A. J.; Attfield, J. P. *Chem. Mater.* **2013,** *25*, 2346-2351.
  Abstract:

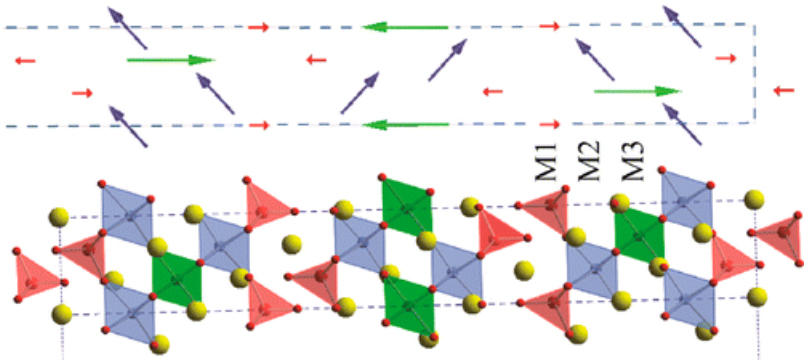

15-layer rhombohedral (15R) $SrCrO_{2.8}$-type superstructures have been discovered in $Sr(Cr_{1-x}Fe_x)O_{3-y}$ perovskites ($0.4 \le x \le 0.6$; space group $R\bar{3}m$; $a \approx 5.56$ and $c \approx 34.6$ Å). Cr/Fe cations are segregated between layers of tetrahedrally and octahedrally coordinated sites. The 15R-$Sr(Cr_{1-x}Fe_x)O_{3-y}$ materials are semiconducting and order ferrimagnetically below 225–342 K. The magnetic structure of an x = 0.5 sample shows spin canting consistent with a simple spin disorder model. Samples with $x \ge 0.7$ have a disordered cubic perovskite structure, and we propose that locally reconstructed (111) planes like those in the 15R materials facilitate oxide ion migration in Cr-based perovskite mixed conductors used in solid oxide fuel cells.

- Hierarchically Structured Nanotubes for Highly Efficient Dye-Sensitized Solar Cells
  Ye, M.; Zheng, D.; Lv, M.; Chen, C.; Lin, C.; Lin, Z. *Adv. Mater.* **2013**, *25*, 3039–3044.

Abstract:

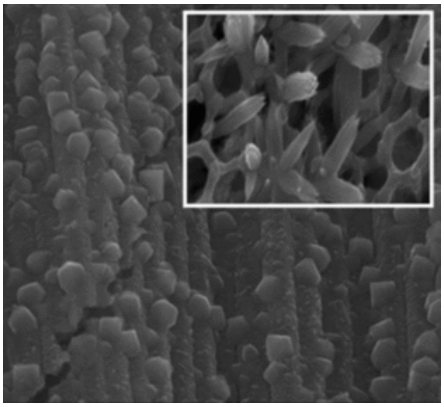

Hierarchical TiO_2 nanotube arrays grown on Ti foil are yielded by subjecting electrochemically anodized, vertically oriented TiO_2 nanotube arrays to hydrothermal processing. The resulting DSSCs exhibit a significantly enhanced power conversion efficiency of 7.24%, which is a direct consequence of the synergy of higher dye loading, superior light-scattering ability, and fast electron transport.

- An All-Optical, Non-volatile, Bidirectional, Phase-Change Meta-Switch
  Gholipour, B.; Zhang, J.; MacDonald, K. F.; Hewak, D. W.; Zheludev, N. I. *Adv. Mater.* **2013**, *25*, 3050–3054.
  Abstract:

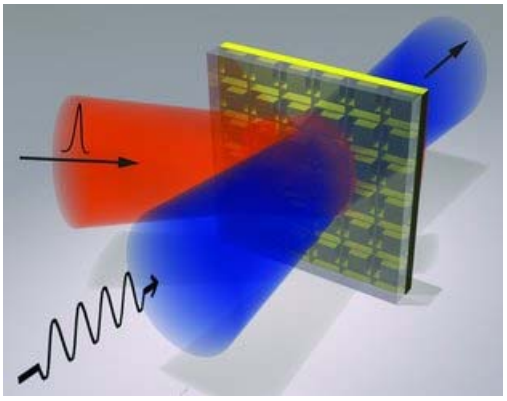

Non-volatile, bidirectional, all-optical switching in a phase-change metamaterial delivers high-contrast transmission and reflection modulation at near- to mid-infrared wavelengths in device structures down to $\approx 1/27$ of a wavelength thick.

- Photothermally Activated Hybrid Films for Quantitative Confined Release of Chemical Species
  Matteini, P. ; Tatini, F. ; Luconi, L. ; Ratto, F. ; Rossi, F. ; Giambastiani, G.; Pini, R. *Angew. Chem. Int. Ed.* **2013**, *52*, 5956–5960.
  Abstract:

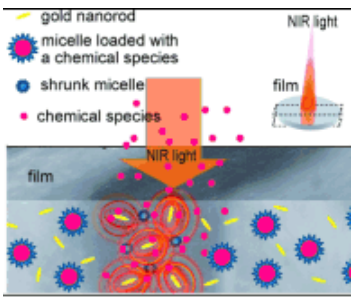

Illuminating films of a porous chitosan matrix containing gold nanorods and thermosensitive micelles loaded with a chemical stimulates local photothermal conversion of the gold nanorods. The heat produced activates the ejection of the chemical from the micelles (see scheme), and causes the transient permeabilization of adjacent cell membranes, resulting in a selective cellular uptake of the released chemical with control over spatiotemporal parameters and dosage.

- Helical Oligomers of Thiazole-Based γ-Amino Acids: Synthesis and Structural Studies
  Mathieu, L. ; Legrand, B.; Deng, C.; Vezenkov, L.; Wenger, E.; Didierjean, C.; Amblard, M.; Averlant-Petit, M.-C.; Masurier, N.; Lisowski, V.; Martinez, J.; Maillard, L. T. *Angew. Chem. Int. Ed.* **2013**, *52*, 6006–6010.
  Abstract:

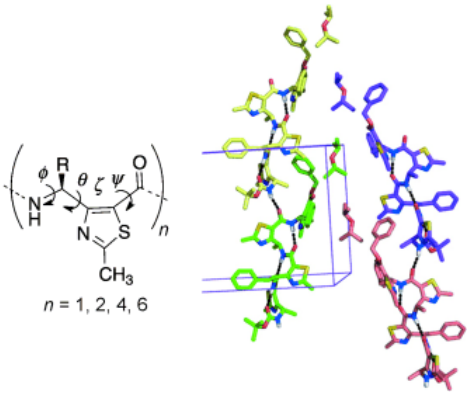

9-Helix: 4-Amino(methyl)-1,3-thiazole-5-carboxylic acids (ATCs) were synthesized as new γ-amino acid building blocks. The structures of various ATC oligomers were analyzed in solution by CD and NMR spectroscopy and in the solid state by X-ray crystallography. The ATC sequences adopted a well-defined 9-helix structure in the solid state and in aprotic and protic organic solvents as well as in aqueous solution.